

# Biophysical Methods for Attomolar Detection of Compounds Acting on Protein Oligomer States

William Lawless<sup>1,2†</sup>, Mark A. Eschenfelder<sup>1†</sup>, Robert P. Sparks<sup>1,2</sup>, Stephanie Krzykowski<sup>1</sup>, Kenyon G. Daniel<sup>1,4</sup>, Wayne C. Guida<sup>1,3\*</sup>

<sup>1</sup> Department of Chemistry; University of South Florida, Tampa, FL, USA.

<sup>2</sup> Research Service; James A. Haley Veterans Hospital, Tampa, FL, USA.

<sup>3</sup> H. Lee Moffitt Cancer Center and Research Institute at the University of South Florida, Tampa, FL, USA.

<sup>4</sup> Department of Molecular Biosciences; University of South Florida, Tampa, FL, USA.

\* Correspondence: Dr. Wayne C. Guida, Department of Chemistry, University of South Florida, CHE 205, 4202 E. Fowler Avenue, Tampa, FL 33620, USA

† These authors contributed equally.

**Keywords:** Microscale thermophoresis, dynamic light scattering, STING, 2',3'-cGAMP, cyclic-di-GMP, clonixeril

**Abstract:** Few protocols exist today that demonstrate repeatable resolution of small molecule interactions with target proteins at extremely low analyte levels, particularly at sub-femtomolar levels. We have developed two approaches for rapid screening and biophysical analysis which leverage changes in protein oligomer states to study highly potent drug candidates. The first protocol employs microscale thermophoresis (MST) to measure competitive disruption of oligomerization following exposure of the target protein to its endogenous ligand. The second protocol engages dynamic light scattering (DLS) to measure the changes in physical size of oligomers after exposure endogenous ligand and/or analyte. We demonstrate the utilization of these methods through measurements of stimulator of interferon genes (STING) exposure to 2',3'-cGAMP and the drug candidate clonixeril along with several analog compounds that were created for lead optimization.

The problem with detection of molecular interactions at extremely low analyte concentrations, such as the attomolar range, is that the ratio between the target protein and the analyte is exorbitantly large (on a ratio scale of millions or billions) or that the sample size needed to be measured would be well under the threshold for most modern detectors. This makes the direct measurement of dissociation constants ( $K_D$ ) extremely difficult or impossible without leveraging the biological function of the target protein itself. Certain proteins are known to undergo oligomerization as part of their biological activity and may form aggregates containing a few all the way up to hundreds of biological units, resulting in a considerable overall increase in mass.(1, 2) Even if a typical oligomer is only formed from a maximum of four or five units, the ratio of mass between an oligomer and its starting monomer is still significant. Some proteins such as stimulator of interferon genes (STING) do not have a known maximum size, and DLS results suggest oligomeric

units achieve a mass larger than the size threshold of the detector.(3, 4) Disruption of these oligomers by small molecules may not require a high concentration and we have predicted and demonstrated models wherein a single small molecule breaks a large chain into two or more parts or enables an unraveling mechanism. It is by this principle that we begin with large oligomerized molecules which are easily measured by thermophoresis detectors or by scattered light instruments, expose them to extremely low analyte concentrations, and measure the resulting disruption of oligomerization.

Microscale thermophoresis (MST) is a technique that measures the interaction between biomolecules (targets) and binders thereof (ligands) by application of a thermal transport force.(4) Particle movement occurs away from the point of heat transference from hot towards cold in a phenomenon known as the Ludwig-Soret effect.(4, 5) The Monolith NT.155 MST instrument uses

embedded software (developed by NanoTemper) that establishes a normalized fluorescence ( $F_{\text{norm}}$ ) value derived from the Soret coefficient, which is a simple calculation of the total fluorescence after thermophoresis divided by the total fluorescence before thermophoresis.(4) Consistent changes in this value reflect changes in the target protein because of one or multiple interactions within a series dilution of analyte.(4) The specific types of changes that affect movement during thermophoresis are direct binding events or changes in mass, conformational changes, change in charge distribution, or change in hydration shell.(4) MST, alone, can determine whether a polymerization or depolymerization event has occurred, but it cannot identify the specific event or combination of events that lead to this end. For this reason, we paired MST with dynamic light scattering (DLS) to affirm that physical changes in the actual oligomer state have taken place.

DLS measures (via Rayleigh scattering) the particle size and distribution within a solution.(6) During experiments, samples are placed in a cuvette, a laser passes through the sample at an instrument specific angle ( $173^\circ$  is commonly used for backscattering), and particle size is estimated in nanometers by application of Rayleigh approximation which states that the intensity of light measured is proportional to  $d^6$  whereas  $d$  is equal to the diameter of the particle.(6, 7) Some fluctuations are known to occur especially with larger particles exiting and entering the pathway of light due to Brownian motion.(7, 8) This is described by the Einstein-Stokes equation which applies to the random thermal movement of molecules in solution:  $D_h = k_B T / 3\pi\eta D_t$ , whereas  $D_h$  is the hydrodynamic diameter which represents the particle size,  $k_B$  is Boltzmann's constant ( $1.380649 \times 10^{-23}$  J/K),  $T$  is the thermodynamic temperature (295K standard),  $\eta$  is the dynamic viscosity of the solution ( $8.90 \times 10^{-4}$  Pa\*s for pure water, notably buffers have varying dynamic viscosities), and  $D_t$  is the translational diffusion coefficient which is found during the light scattering measurement.(7) (6, 9) A polydisperse solution is defined as a solution which contains particle sizes of varying size, shape, and mass.(7, 10) Size is obtained from the correlation function for polydisperse solutions  $G(\tau) = A[1+B g_1(\tau)^2]$  whereas  $A$  is the baseline for the correlation function,  $B$  is the intercept of the correlation function, and  $g_1(\tau)^2$  is the sum of exponential decays contained within the monodisperse function  $G(\tau) =$

$A[1+B \exp(-2 \Gamma \tau)]$  whereas  $\Gamma = D_t q^2$ , where  $q$  is the scattering vector given by the formula  $q = (4\pi n/\lambda)\sin(\theta/2)$ ;  $n$  is the refractive index,  $\lambda$  is the wavelength, and  $\theta$  is the angle of light scatter,  $D_t$  is determined by using the Stokes-Einstein equation, and  $\tau$  is the time difference of the measurements within the correlogram.(7, 11) Multiple values are obtained over timepoints to generate a Z-Average, which is defined as the harmonic intensity averaged particle diameter, and an estimation of the width of dispersion, referred to as the polydispersity index.(7)

We demonstrate the use of these protocols using STING which is one of the main mediators in innate immunity within mammalian cells.(12-16) STING is activated by the endogenous signaling molecule cyclic GMP-AMP (cyclic (guanosine- (2'  $\rightarrow$  5')-monophosphate- adenosine- (3'  $\rightarrow$  5')-monophosphate) or 2',3'-cGAMP) that is produced in response to detection of cytosolic nucleic acids by cyclic GMP-AMP synthase (cGAS).(12, 13) STING signaling is derived from the formation of oligomeric structures.(14) STING is an endoplasmic reticulum (ER) transmembrane protein and oligomer formation within the ER is directly caused by binding of 2',3'-cGAMP that induces a conformational change enabling lateral stacking of STING dimers.(15) This oligomeric state serves to align phosphorylation sites when binding to TANK-binding kinase 1 (TBK1), which is required for phosphorylation of interferon regulatory factor 3 (IRF3) that drives type 1 interferon expression.(3, 16)

Clonixeril (**Supplemental Figure 1A**) is a highly potent partial agonist, which demonstrates properties of both a weak agonist and a potent antagonist of the STING receptor in both the presence and absence of 2',3'-cGAMP. Following a luciferase reporter assay using wild type THP-1 cells in which the concentration was progressively lowered to near zero, it was discovered that clonixeril had the ability to effect pIRF3 production at high attomolar concentrations.(17) We sought to develop a cost- and time-effective option for first line screening of biotarget-ligand interactions during lead optimization efforts.

## Results

### Microscale Thermophoresis Protocol

MST is analyzed using the Soret coefficient  $S_T = F_{\text{norm}} = c_{\text{hot}}/c_{\text{cold}} = \exp(-S_T \Delta T)$ .(4) The  $EC_{50}$ , or 50% of the effective concentration to cause a change, is then derived from fitting a quadratic formula to the

fluorescent function, resulting in a nonlinear regression curve.(4) The measurement of these values requires a steady-state, which is achieved by ensuring that both the target protein and analyte are completely solubilized within the same solution. There is no universal solvent with or without surfactant for all proteins and so the manufacturer of the MST instrument (i.e. NanoTemper) has included useful software designed for empirical determination and comparison of solubility during thermophoresis.(4) The following guidelines should be considered when determining a buffer strategy: 1) no more than 5% DMSO should be used because greater amounts result in randomized target drifting that is not related to thermophoresis; 2) organic solvents (e.g., methanol, ethanol, acetonitrile, etc.) should be limited because excessive amounts restrict statements that can be made about the natural state of biological proteins and may also effect conformational changes and/or denature the protein itself; and 3) the use of surfactant should be limited to less than the critical micelle concentration for individual surfactants as greater amounts may interfere with the interaction between target and analyte.(18) We determined empirically that the use of a HEPES buffer with the P20 surfactant (HBS-P) provided the best solubility for the STING protein and analyte compound together through several trials using the same components as the protocol validation process (data not shown).

Most fluorescent markers used for MST are chelated to the target protein using a nickel ( $\text{Ni}^{2+}$ ) ion complexed to a histidine residue.(4) Proteins are often modified to include a repeating histidine (6 or 8 residues) tag for chelation, but it is notable that a successful chelation and detection may occur with a protein so long as it contains a non-sterically hindered histidine residue on the outer surface of its tertiary structure and binding of a fluorescent compound to this location does not interfere with small molecule interactions, conformational changes, and/or oligomerization.(19, 20) Dye concentration should be limited to a molar ratio equal to less than that of the target protein, and is typically held at 50% or 75%, because unbound dye moves much more rapidly during thermophoresis than target protein bound to dye and can significantly interfere with measurements.(4) MST instruments are designed to detect fluorescence in either the blue or the red channel.(4) The excitation wavelength is 600-650 nm for the red channel and 460-490 nm for

the blue channel.(4) The wavelength for the blue channel covers the excitation wavelength necessary for measurement of GFP proteins, although we find that the concentration of target protein tagged with GFP required for the detector is far higher than that needed for fluorescence dyes, and this concentration increase added to the additional mass of a GFP unit may cause steric issues during thermophoretic movement (**Supplemental Figure 2**). According to these data, a GFP protein concentration between 87  $\mu\text{M}$  and 326  $\mu\text{M}$  would be required for detection, and may result in reduced experimental sensitivity.(21) NanoTemper offers a variety of fluorescent markers for sale, all of which specifically exploit the red channel. We performed the MST protocol using Atto-488 (Abcam, USA), a blue channel nickel chelation dye that complexes with histidine residues.

The use of transmembrane proteins in assays such as MST or DLS present a multitude of challenges directly relating to intramolecular interactions and often need to be paired with a hydrophobic vehicle such as nanodiscs.(22, 23) The carboxyl terminal domain (CTD) of STING is highly conserved across multiple species and according to crystal structure data, it has been shown to function independently of its transmembrane domain, both in conformational change and oligomerization.(24) We recommend the use of truncated variants only when protein functionality is conserved.

Several limitations currently exist in the NanoTemper software: 1) a 1:10 dilution series is not supported in the auto-fill section and therefore must be manually entered; 2) ligand concentrations entered below a molarity of  $1 \times 10^{-15}$  (femto-) do not generate normalized fluorescent values within the analysis software. This causes the need to track analyte concentration values separately from the software and apply them to the results in third party software, and 3) analysis software cannot automatically process more than one nonlinear regression curve that exists in a single data set. In the case where a protein is showing biphasic or multiple valid points of change in  $F_{\text{norm}}$ , values have to be manually discarded within the analysis software or the data has to be exported as raw values and entered into a separate program for analysis (i.e. GraphPad Prism).

### Example of MST Protocol

1. Mix STING R232 variant (human recombinant; 138-379) protein at 200 nM in HBS-P buffer

(0.01 M HEPES pH 7.4, 0.15 NaCl, 0.005% v/v surfactant P20) with 100 nM 2',3'-cGAMP and 100 nM of NTA-Atto 488 dye (blue; nitrilotriacetic acid complexed to Ni<sup>2+</sup> - ion).

2. Cover samples from light and incubate for 1 hour at room temperature (25°C) to induce oligomerization and dye the target protein.
3. Centrifuge at 400 x g for 10 minutes to remove large aggregates within the solution.
4. Prepare a series dilution of the desired concentration range using HBS-P with 0-5% DMSO in a separate plate or series of tubes. The amount of DMSO will depend on analyte solubility but should not exceed 5% DMSO.
5. Add the dyed protein mixture to each analyte sample in a 1:1 ratio. Note the initial concentration of both the starting material and the samples should be at 2X prior to this point.
6. Incubate for 15 minutes to allow reaction to occur or start measurements immediately.
7. Set up the program using the blue detection channel with excitation power set to 100% and MST set to high allowing 3 s prior to MST ON to check for initial fluorescence differences, 30 s - 35 s for thermophoresis, and 3 s for regeneration after MST OFF.
8. Load samples into capillaries and run the program.
9. Repeat samples at 30 and 45 minutes to evaluate interaction over time or repeat assay at a single time point to better estimate the error.

### Dynamic Light Scattering Protocol

DLS is designed to estimate the size of any particles within a solution using nanometer as the base unit of measurement.(7) The technique is extremely sensitive to contamination and/or intramolecular aggregation and therefore will not differentiate between particles. For this reason, it is imperative that all aqueous reagents used in DLS are filtered. A 3 kDa centrifuge filter is recommended to be used for buffer solutions since this aperture does not disrupt the integrity of the buffer and removes particles that are large enough to be detectable by the instrument, with consideration that proteins less than 3 kDa are estimated to be less than 1 nm in size.(25) This should be performed even if the buffer was diluted or solubilized from sterile stock using purified or prefiltered media as microaggregates may still be present within the buffer. It is also strongly recommended that the target protein be purified in a

similar manner prior to the initiation of oligomerization, especially in proteins known to undergo spontaneous aggregation or auto-oligomerization for the purpose of ensuring the same or statistically similar particle distribution during a starting point for each experiment. Aperture size should be selected and verified based on the size of the target protein. For the variant of STING used in the development of this protocol (36 kDa), we found that a 100 kDa centrifuge filter was effective at creating a starting solution containing only biological monomers, which was verified by DLS measurements taken from controls compared to width measurements of STING made using x-ray crystallography data.(26)

The following strategy can be used to reduce error caused by signal fluctuation as a result of Brownian motion with large particles: (1) employ as many short measurements as is reasonably possible and average these measurements over time. The number of measurements and the time required will vary based on how rapidly the target protein achieves equilibrium; and (2) restrict sample size to as small as possible to alleviate both the maximum size that an oligomer may achieve within a molar solution and to reduce the space given for any particle to move.

It was statistically determined based on the Law of Large Numbers that all data gathered for the STING project from time zero repeatably converges when data are averaged over a minimum of 960 one-second measurements (Figure 2A and Supplemental Figure 3A-F).(27, 28) This convergence is probably unique to STING analysis under the parameters given within this experiment and other proteins will likely need to be empirically evaluated to determine length of convergence. It's not recommended that the reaction time that occurs before the period of equilibrium be removed because some analyte compounds noticeably act on the protein at much slower rates and this factor should be averaged into the whole for comparison against control.

### Example of DLS Protocol

1. Centrifuge buffer in 3 kDa centrifuge filter at 400 x g for 5 minutes. Discard flowthrough.
2. Place filter in a fresh centrifuge tube. Centrifuge at 400 x g for 10 to 15 minutes.
3. Place filtered buffer into 100 kDa centrifuge filter (or appropriate size for the monomer of

- protein being used) and centrifuge at 400 x g for 3 minutes. Discard flowthrough.
- Mix filtered buffer in with target protein and place into 100 kDa centrifuge filter. Centrifuge at 400 x g for 3 minutes.
  - Measure concentration on nanodrop using the proper extinction coefficient.
  - Dilute protein sample and endogenous ligand to 200 nM in separate aliquots using filtered buffer. Dilute analytes to 2X target concentration. Store samples on ice.
  - Setup the run program on the instrument to include 40 measurements at 1 sec/measurement and 24 runs.
  - Mix 20  $\mu\text{L}$  analyte with 10  $\mu\text{L}$  endogenous ligand and 10  $\mu\text{L}$  protein in polystyrene low volume cuvette.
  - Ensure the cuvette is clean of dust or particles on the outside of the casing, place cuvette into the instrument and start the program.

### MST is Validated by 2',3'-cGAMP

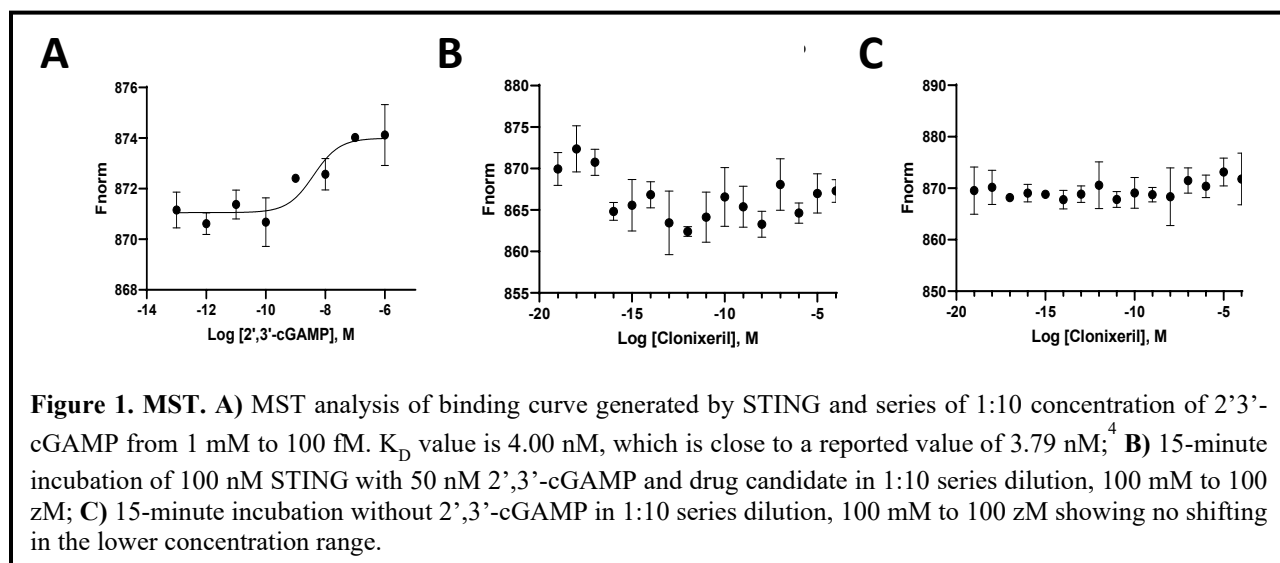
The validation of the MST protocol was based on reported experimental isothermal calorimetry (ITC) results regarding the interaction between the truncated STING R232 variant and 2',3'-cGAMP. It was established that 2',3'-cGAMP binds to STING with a  $K_D$  of 3.79 nM.<sup>(15)</sup> We aimed to verify that the MST protocol could repeat this  $K_D$  value within error using a 1:10 dilution series and additionally use the data to validate the concentration of 2',3'-cGAMP that we used in our competition assay.

To examine this, we constructed a 1:10 titration series for 2',3'-cGAMP from 1 mM to 10 fM, which

resulted in an experimental  $K_D$  on MO.Affinity Analysis software (NanoTemper) of 4.0 nM (**Figure 1A**).<sup>(4)</sup> This more than agrees with the standard margin of error for MST runs which is established as plus or minus one order of magnitude.<sup>(29)</sup> A concentration of 50 nM for 2',3'-cGAMP was selected, which represents a ten-fold increase over the experimentally measured  $K_D$  value of its interaction with STING and therefore enables the maximum number of oligomers to form under standard conditions.<sup>(15, 30)</sup>

### Oligomerization is Required for MST Resolution

A series of three assays were run using the 15-minute incubation as the repeat timepoint with and without 50 nM 2',3'-cGAMP. The goal was to examine whether the presence of 2',3'-cGAMP and thus STING oligomeric compounds are necessary to see high affinity interactions with STING against clonixeril. The results demonstrate that no shifting occurs within the high affinity area when 2',3'-cGAMP is not present (**Figure 1B-C**). We interpret this to mean that 2',3'-cGAMP is required for resolution by MST at these low concentration levels because it enables the presence of STING oligomeric structures, and the breakdown of these structures creates a significant size difference between species to be detectable by MST. This claim was explored by DLS and is supported by data presented in **Figure 2C**. A decrease in  $F_{\text{norm}}$  signal as concentration of clonixeril increases suggests more rapid movement during thermophoresis, likely indicating less mass due to the breakdown in these structures. Importantly, this does not mean that there is no





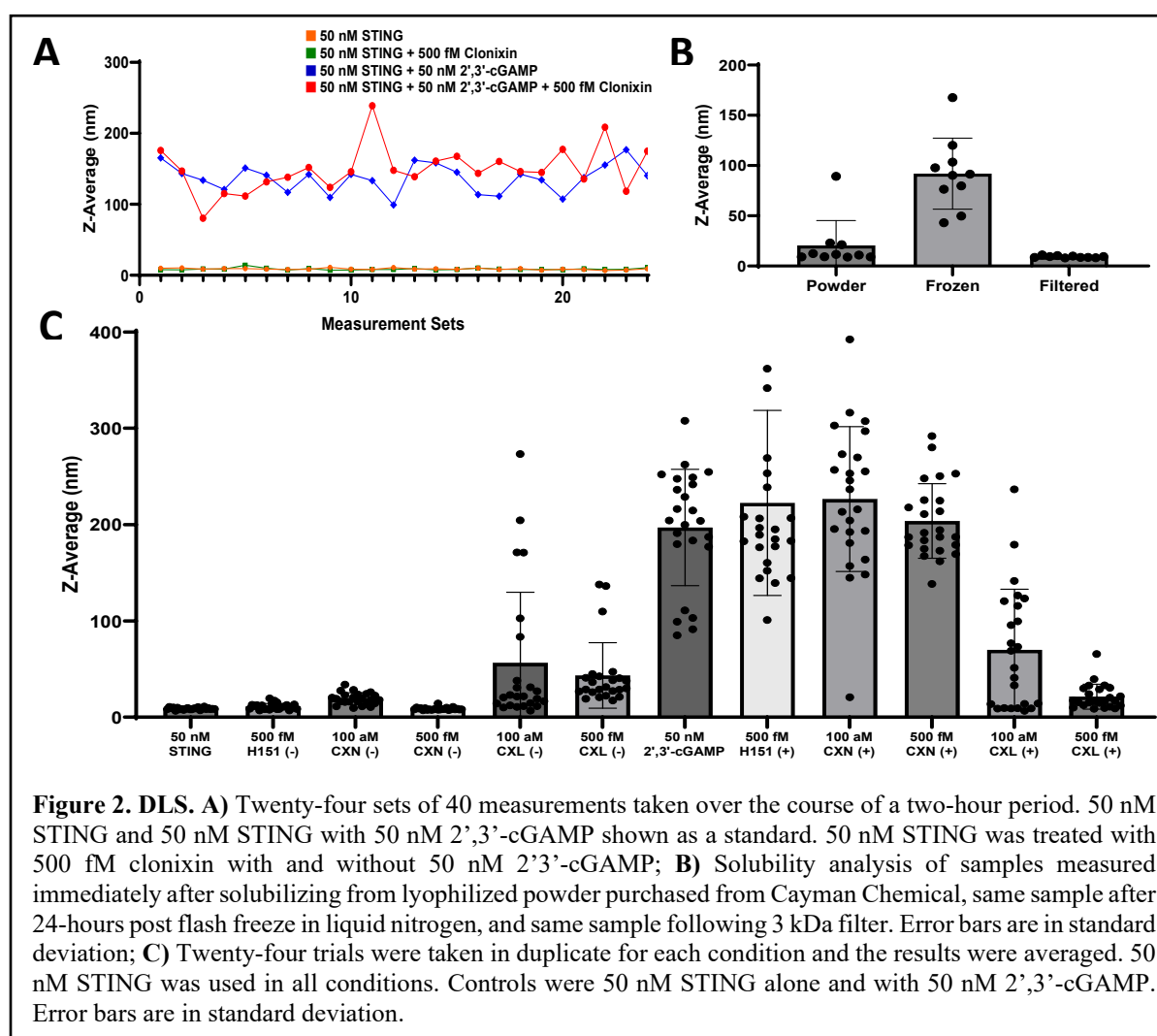
interaction between clonixeril and STING at extremely low concentration in the absence of 2',3'-cGAMP, but the oligomers formed from these interactions are not significant enough to cause a measurable difference in MST.

### DLS Measures Oligomeric Disposition

We designed the initial protocol for DLS to take a magnitude of measurements to gain kinetic insight on oligomer properties in real time. However, it was quickly discerned that STING oligomers are rapidly formed or deconstructed at rates which cannot be reliably measured by this protocol (**Figure 2A and Supplemental Figure 3A-F**). We instead focused on measuring the equilibrium of the oligomer states. Within the first set of trials, we discovered that STING had a propensity to form at least a minor number of aggregates when stored at  $-80^{\circ}\text{C}$ , regardless of the speed at which the samples were frozen or thawed (**Figure 2B**). These aggregates

needed to be removed using a 100 kDa centrifuge filter to establish the same starting point and to significantly stabilize the fluctuation of the Z-Average over the period of the experiments.

The angstrom size of a biological unit monomer of the CTD domain of human STING has been measured by x-ray crystallography to be approximately 47-54 Å in the open conformation and 34-35 Å in the closed conformation.(26) This gives an average diameter of approximately 4 nm per biological unit or 8 nm with an attached SUMO tag and is precisely what we measure in the absence of 2',3'-cGAMP (**Figure 2C**). With 2',3'-cGAMP present, the Z-Average fluctuates due to Brownian motion but averages out at approximately 200 nm. Clonixin is not known to either induce or inhibit STING oligomerization with or without the presence of 2',3'-cGAMP and therefore is shown as a negative control (**Figure 2A**). We used compound H151



(Supplemental Figure 1B) to demonstrate a second negative control since it is a known palmitoylation agent that covalently binds to full length STING at C91, and this residue does not exist in our truncated STING variant.

To examine the effect of small molecules on the oligomer state of STING, 50 nM STING was exposed to 100 nM or 500 nM analyte with and without 50 nM 2',3'-cGAMP in duplicate trials. Results were compared to 50 nM STING alone and 50 nM STING exposed to 50 nM 2',3'-cGAMP (Figure 1E).

Results demonstrate that clonixeril causes a minor amount of STING oligomerization without 2',3'-cGAMP present and significantly disrupts oligomers formed with 2',3'-cGAMP. The major disruption caused when 2',3'-cGAMP is present is likely the reason that we can measure a shift in  $F_{norm}$  during MST. We hypothesize the reason for this activity to be that clonixeril induces a conformational change in STING that results in oligomerization which is different and not compatible with oligomers formed because of interaction with 2',3'-cGAMP.

## Discussion

We report the development of MST and DLS protocols that demonstrate the ability to detect interactions within the sub-femtomolar concentration range. We assert based on the evidence presented that these protocols would work with any protein that undergoes oligomerization as part of their natural biological mechanism and that these protocols would demonstrate rapid interaction with small molecules which either cause or disrupt oligomerization. The disruption of oligomeric structures can be seen clearly on MST and DLS within the high affinity range and easily measured by nonlinear regression curves for the estimation of a  $K_D/EC_{50}$  value or measured for size by light scattering. Further, both protocols are low cost, rapid, and provide a basis for gathering initial evidence of interactions with oligomeric proteins.

There is a higher fluctuation between individual samples within the MST results due to the nature in which STING undergoes oligomerization to form structures containing varying biological units. This leads directly to a slightly larger error between samples than is typically experienced with MST and other targets, because of the direct inability to pipette exactly the same number of base units that makes up

the oligomer species in each sample. In our experiments, we stabilized this variation by maintaining an equal amount of STING in each sample. The error that remains was not large enough to offset the shift in  $F_{norm}$  and results can be confirmed by examination of the inflection curve by statistical analysis. It is unknown whether this is a significant factor using other proteins that undergo oligomerization.

The MST trendline should be linear until an inflection and then linear again after the inflection unless in rare cases there are multiple points of inflection such as shown in Figure 1A. Some points in MST experiments may also sometimes deviate drastically from the trendline. These outlying points can be statistically removed from the set using a two-tailed T-test or a Grubb's test whereas the trendline at that point represents the sample mean and  $N$  is equal to 1. For this reason, it is highly recommended that at least two linear points exist after an inflection, or optimally three linear points, for the result to be considered statistically significant.

Data concerning all analog compounds generated from the clonixeril and clonixin base structure will be reported in a later publication. Importantly, not all compounds showed interaction with STING, general functional groups demonstrated similar trends, and the overall set indicates a wide range of  $EC_{50}$  interactions with STING. These methods demonstrate a high degree of experimental reproducibility and all compounds have reproduced statistically the same results *in vivo* and *in vitro*.

We further predict that these protocols would be of enormous utility in the qualitative and statistical analysis of other proteins for which oligomerization is an integral component of a cellular signal transduction event, exemplified by pathways involving immune function.<sup>(31)</sup> We are confident that our observations with STING may be repeated in multiple other pathways, and analysis using methods such as the ones described in this publication may lead to the discovery of highly potent drug candidates.

## References

1. G. Shang, C. Zhang, Z. J. Chen, X.-c. Bai, X. Zhang, Cryo-EM structures of STING reveal its mechanism of activation by cyclic GMP-AMP. *Nature* **567**, 389-393 (2019).

2. K. Hashimoto, A. R. Panchenko, Mechanisms of protein oligomerization, the critical role of insertions and deletions in maintaining different oligomeric states. *Proceedings of the National Academy of Sciences* **107**, 20352-20357 (2010).
3. C. Zhang *et al.*, Structural basis of STING binding with and phosphorylation by TBK1. *Nature* **567**, 394-398 (2019).
4. NanoTemper (2023) User Manual Monolith NT.115.
5. S. Duhr, D. Braun, Why molecules move along a temperature gradient. *Proceedings of the National Academy of Sciences* **103**, 19678-19682 (2006).
6. J. Stetefeld, S. A. McKenna, T. R. Patel, Dynamic light scattering: a practical guide and applications in biomedical sciences. *Biophys Rev* **8**, 409-427 (2016).
7. M. Instruments (2023) Dynamic Light Scattering: An Introduction in 30 Minutes.
8. P. A. Hassan, S. Rana, G. Verma, Making Sense of Brownian Motion: Colloid Characterization by Dynamic Light Scattering. *Langmuir* **31**, 3-12 (2015).
9. E. T. Parker, P. Lollar, Measurement of the Translational Diffusion Coefficient and Hydrodynamic Radius of Proteins by Dynamic Light Scattering. *Bio Protoc* **11**, e4195 (2021).
10. T. Tanaka, Quasielastic Light Scattering from Polydisperse Polymer Solution. *Journal of the Physical Society of Japan* **37**, 575 (1974).
11. D. E. Koppel, Analysis of Macromolecular Polydispersity in Intensity Correlation Spectroscopy: The Method of Cumulants. *The Journal of Chemical Physics* **57**, 4814-4820 (1972).
12. L. Sun, J. Wu, F. Du, X. Chen, Z. J. Chen, Cyclic GMP-AMP Synthase Is a Cytosolic DNA Sensor That Activates the Type I Interferon Pathway. *Science* **339**, 786-791 (2013).
13. A. Ablasser, Z. J. Chen, cGAS in action: Expanding roles in immunity and inflammation. *Science* **363**, eaat8657 (2019).
14. H. Shi, J. Wu, Z. Chen, C. Chen, Molecular basis for the specific recognition of the metazoan cyclic GMP-AMP by the innate immune adaptor protein STING. *Proceedings of the National Academy of Sciences of the United States of America* **112** (2015).
15. X. Zhang *et al.*, Cyclic GMP-AMP Containing Mixed Phosphodiester Linkages Is An Endogenous High-Affinity Ligand for STING. *Molecular Cell* **51**, 226-235 (2013).
16. B. Zhao *et al.*, Structural basis for concerted recruitment and activation of IRF-3 by innate immune adaptor proteins. *Proceedings of the National Academy of Sciences* **113**, E3403-E3412 (2016).
17. R. P. Sparks *et al.*, Discovery of Clonixeril as a Sub-Femtomolar Modulator of the Human STING Receptor [Manuscript submitted for publication] (2024).
18. D. R. Perinelli *et al.*, Surfactant Self-Assembling and Critical Micelle Concentration: One Approach Fits All? *Langmuir* **36**, 5745-5753 (2020).
19. N. Soh, Selective Chemical Labeling of Proteins with Small Fluorescent Molecules Based on Metal-Chelation Methodology. *Sensors (Basel)* **8**, 1004-1024 (2008).



20. J. Lotze, U. Reinhardt, O. Seitz, A. G. Beck-Sickinger, Peptide-tags for site-specific protein labelling in vitro and in vivo. *Molecular BioSystems* **12**, 1731-1745 (2016).
21. J. M. Rainard, G. C. Pandarakalam, S. P. McElroy, Using Microscale Thermophoresis to Characterize Hits from High-Throughput Screening: A European Lead Factory Perspective. *SLAS Discov* **23**, 225-241 (2018).
22. S. Kovachka, P. Soule, I. Mus-Veteau, Microscale Thermophoresis to Evaluate the Functionality of Heterologously Overexpressed Membrane Proteins in Membrane Preparations. *Methods Mol Biol* **2507**, 445-461 (2022).
23. R. I. Reis, I. Moraes, Probing Membrane Protein Assembly into Nanodiscs by In Situ Dynamic Light Scattering: A(2A) Receptor as a Case Study. *Biology (Basel)* **9** (2020).
24. S. Ouyang *et al.*, Structural analysis of the STING adaptor protein reveals a hydrophobic dimer interface and mode of cyclic di-GMP binding. *Immunity* **36**, 1073-1086 (2012).
25. H. P. Erickson, Size and shape of protein molecules at the nanometer level determined by sedimentation, gel filtration, and electron microscopy. *Biol Proced Online* **11**, 32-51 (2009).
26. S. L. Ergun, D. Fernandez, T. M. Weiss, L. Li, STING Polymer Structure Reveals Mechanisms for Activation, Hyperactivation, and Inhibition. *Cell* **178**, 290-301.e210 (2019).
27. O. C. Ibe, "1 - Basic Concepts in Probability" in Markov Processes for Stochastic Modeling (Second Edition), O. C. Ibe, Ed. (Elsevier, Oxford, 2013), <https://doi.org/10.1016/B978-0-12-407795-9.00001-3>, pp. 1-27.
28. W. L. Dunn, J. K. Shultis, "Appendix B - The Weak and Strong Laws of Large Numbers" in Exploring Monte Carlo Methods (Second Edition), W. L. Dunn, J. K. Shultis, Eds. (Elsevier, 2023), <https://doi.org/10.1016/B978-0-12-819739-4.00020-2>, pp. 497-500.
29. Anonymous (Monolith NT.115 Series).
30. S. Liu *et al.*, The mechanism of STING autoinhibition and activation. *Mol Cell* **83**, 1502-1518.e1510 (2023).
31. S. Xia, Z. Chen, C. Shen, T. M. Fu, Higher-order assemblies in immune signaling: supramolecular complexes and phase separation. *Protein Cell* **12**, 680-694 (2021).

## Methods

### Materials

STING R232 variant (human recombinant) protein (catalytic domain only, 138-379 N-terminal truncation; purified from *E. coli*) and 2',3'-cGAMP sodium salt was purchased from Cayman Chemical (USA). HST-hSTING variant (human recombinant) protein (catalytic domain only, 155-343 N-terminal truncation with His-SUMO-TEV; plasmid from Dr. Leemor Joshua-Tor, Cold Spring Harbor; purified from *E. coli*) was produced by order from Dr. Kathy Yang at Moffitt Cancer Center. Dimethyl sulfoxide (DMSO), NTA-Atto 488 (blue; nitrilotriacetic acid complexed to Ni<sup>2+</sup> - ion, Na, Na-bis[carboxymethyl]-L-lysine), and NTA-Atto 647 N (red; nitrilotriacetic acid complexed to Ni<sup>2+</sup> - ion, Na, Na-bis[carboxymethyl]-L-lysine) were purchased from Sigma Aldrich (USA). HBS-P buffer (0.01M HEPES pH 7.4, 0.15 NaCl, 0.005% v/v surfactant P20) was purchased from Thermo Fisher Scientific (USA). Monolith NT.115 capillaries were purchased from NanoTemper Technologies (USA). Disposable low volume cuvettes were purchased from Malvern Panalytical (ZEN0118, USA).

### **Microscale Thermophoresis (MST)**

STING R232 variant (human recombinant) protein was solubilized at 200nM in HBS-P (0.01M HEPES pH 7.4, 0.15 NaCl, 0.005% v/v surfactant P20) along with 100 nM 2',3'-cGAMP. 100 nM of NTA-Atto 488 dye (blue; nitrilotriacetic acid complexed to Ni<sup>2+</sup> - ion) is added and incubated for 1 hour at RT covered from light. The resulting mixture was centrifuged at 12,000 x RPM 10 minutes prior to use. A 1:10 series dilution from 200mM to 200zM was created using HBS-P with 1% DMSO. The dyed STING/2',3'-cGAMP mixture was added to each sample in a 1:1 ratio, resulting in a static 100 nM STING, 50 nM 2',3'-cGAMP, and a concentration range from 100 mM to 100 zM. Samples were incubated for 15-minutes prior to loading into Monolith NT.115 capillaries and run on NanoTemper Pico instrument. Samples were run again at 30- and 45-minutes. Detection of the protein was performed using the blue detection channel with excitation power set to 100% and MST set to high allowing 3 s prior to MST on to check for initial fluorescence differences, 35 s for thermophoresis, and 3 s for regeneration after MST off. Analysis was performed using M.O. Affinity Analysis Software with difference between initial fluorescence measured in the first 5 s as compared with thermophoresis at 30 s at 16 different analyte concentrations ranging from 100 mM to 100 zM and exported into Graphpad Prism v.8 using a Log inhibitor versus response for parameter fit.

### **Dynamic Light Scattering (DLS)**

STING R232 variant (human recombinant) protein or HST-hSTING variant (human recombinant) protein was filtered using a 100 kDa centrifuge filter and solubilized at 200nM in HBS-P (0.01M HEPES pH 7.4, 0.15 NaCl, 0.005% v/v surfactant P20). Ext. coefficient used for His-SUMO-STING was 24870 M<sup>-1</sup> cm<sup>-1</sup>. Measurements were made using a Malvern Zetasizer Nano ZS set to 40 measurements at 1 s/measurement and 24 runs. Samples were created using 20 µL analyte with 10 µL protein and 10 µL 200 nM 2',3'-cGAMP or buffer into a disposable low volume cuvette.

### **Acknowledgements:**

We thank University of South Florida Chemical Purification, Analysis, and Screening Core and H. Lee Moffitt Cancer Center and Research Institute

Chemical Biology Core. We additionally thank Dr. James Leahy and Dr. Jamie Nunziata (Chemistry Department, USF) for the synthesis of the clonixeril and clonixin analogs and for insight which lead to the development of the protocol, Dr. Yu Chen (Molecular Medicine Department, USF) for his generous gift of centrifuge filters, and Dr. Edward Turos for use of his Malvern DLS instrument. We thank Dr. Leemor Joshua-Tor, Cold Spring Harbor for her generous gift of STING-CTD plasmids.

### **Funding:**

This work was supported in part by The National Institutes of Health, National Institute for Allergy and Infectious Disease, R21AI149450. "Development of antagonists targeting STING in systemic lupus erythematosus," 01/2020 – 12/31/2021 and in part by IBIS Therapeutic LLC. We thank them for their generous support.

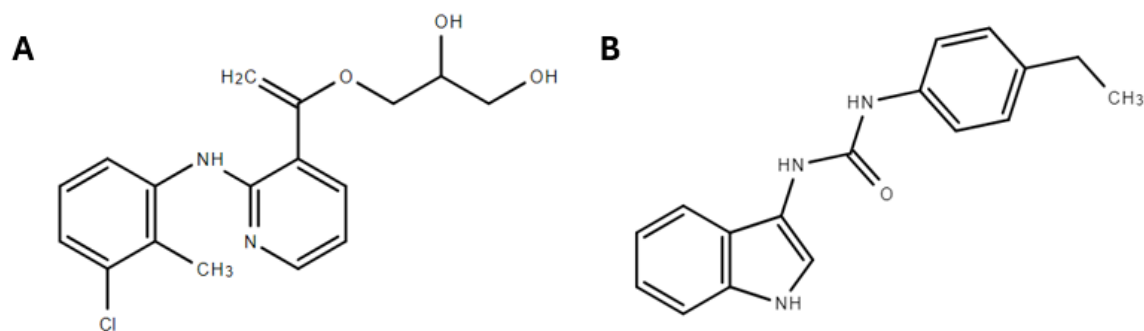
### **Author Contributions:**

WL drafted the manuscript. All authors read and approved the final manuscript.

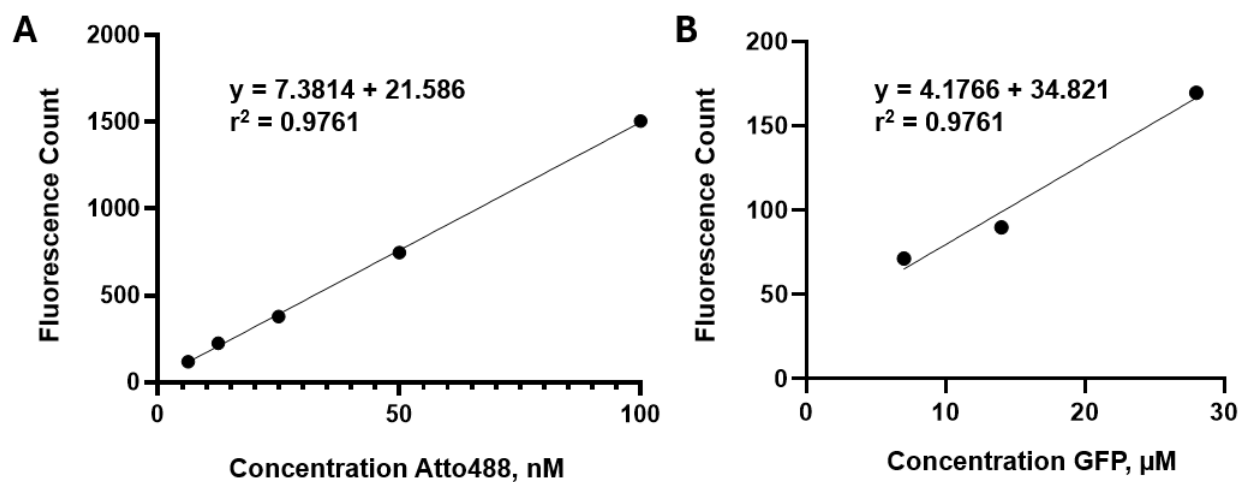
### **Conflicts of interest:**

Wayne C. Guida has a financial interest in IBIS Therapeutics. Patent WO2021042024A1, STING modulators, compositions, and methods of use. 2020. Wayne C. Guida and Robert P. Sparks.

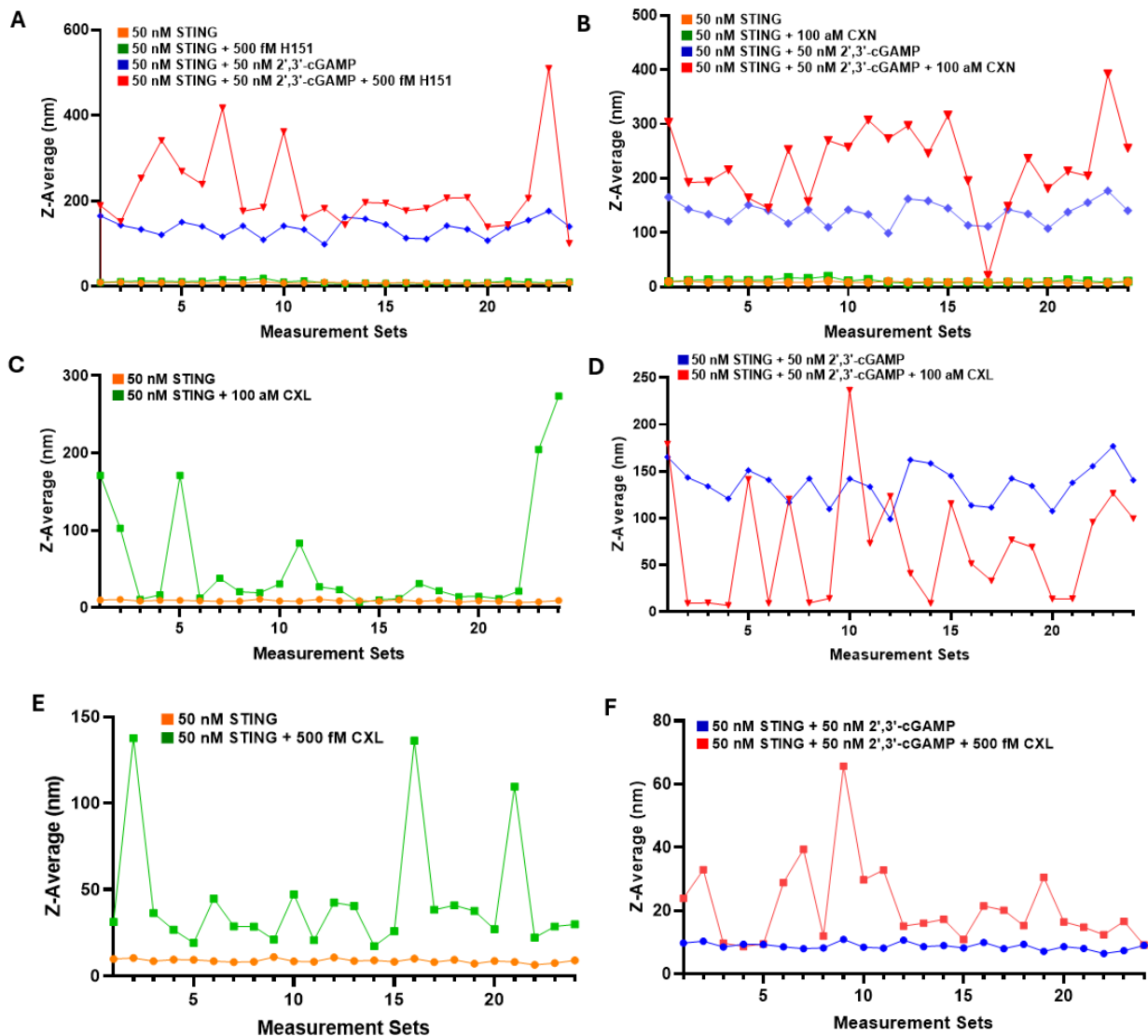
su



**Supplemental Figure 1.** Chemical structures for **A)** Clonixeril; and **B)** H-151.



**Supplemental Figure 2.** Series dilutions for MST fluorescence count. **A)** 50 nM STING exposed to 1:1 series dilution Atto488 dye from concentrations 100 nM to 6.25 nM; **B)** GFP purified protein in 1:1 series dilution from concentration 28 μM to 7 μM.



**Supplemental Figure 3. DLS** Twenty-four sets of 40 measurements taken over the course of a two-hour period. 50 nM STING and 50 nM STING with 50 nM 2',3'-cGAMP shown as a standard. **A)** 50 nM STING was treated with 500 fM H151 with and without 50 nM 2',3'-cGAMP; **B)** 50 nM STING and 50 nM STING with 50 nM 2',3'-cGAMP shown as a standard. 50 nM STING was treated with 100 aM CXN with and without 50 nM 2',3'-cGAMP; **C)** 50 nM STING shown as a standard. 50 nM STING was treated with 100 aM CXL without 50 nM 2',3'-cGAMP; **D)** 50 nM STING with 50 nM 2',3'-cGAMP shown as a standard. 50 nM STING was treated with 100 aM CXL with 50 nM 2',3'-cGAMP; **E)** 50 nM STING shown as a standard. 50 nM STING was treated with 500 fM CXL without 50 nM 2',3'-cGAMP; **F)** 50 nM STING with 50 nM 2',3'-cGAMP shown as a standard. 50 nM STING was treated with 500 fM CXL with 50 nM 2',3'-cGAMP.